Aerodynamic aspects of the sealing of gas-turbine rotor-stator systems

Part 3: The effect of nonaxisymmetric external flow on seal performance

U. P. Phadke
Scientific Generics, King's Court, Cambridge CB4 2PF, UK

J. M. Owen
School of Engineering and Applied Sciences, University of Sussex, Falmer, Brighton, Sussex BN1 9QT, UK

Received 3 April 1987 and accepted for publication on 29 June 1987

The effect of a nonaxisymmetric external flow on the sealing performance of a shrouded rotor-stator system has been studied using flow visualization and pressure measurements. When ingress occurred, ingested fluid moved transversely across the wheel space from regions of high to low pressure in the external-flow annulus. One of the four seal geometries tested contained a double-shrouded seal, and the inner shroud attenuated the external pressure asymmetries so that most of the ingested fluid was confined to the space between the shrouds. Six different circumferential variations of pressure were used to separate the effects of flow rate and pressure asymmetry, and it was found that, for all four seals, the minimum sealing-flow rate necessary to prevent ingress could be correlated with the maximum circumferential pressure difference measured in the external-flow annulus.

Keywords: sealing; rotating disks; rotor-stators

Introduction

Studies of ingress in a number of different shrouded rotor-stator systems were reported in Parts 1 and 2 (these parts, Refs. 1 and 2, are referred to here as I and II) for the case where the external flow was either zero or quasi-axisymmetric. It was shown that at small values of Re_w/Re_θ (where Re_w and Re_θ are the external-flow and rotational Reynolds numbers, respectively) there is rotation-dominated regime where $C_{w,min}$, the minimum sealing-flow rate necessary to prevent ingress, increases with increasing Re_θ. At large values of Re_w/Re_θ, there is an external-flow-dominated regime in which $C_{w,min}$ is proportional to Re_w but is virtually independent of Re_θ.

For the tests reported in II, perfect axisymmetry of the external flow was not achieved. As the small variations in circumferential pressure increased with increasing Re_w, it was not possible to conclude whether the results for the external-flow-dominated regime were caused by Re_w or by the pressure asymmetries. It is the object of the work reported below to determine which of these effects causes ingress.

Of the seven geometries tested in I, seals 1, 2, 3, and 5 were examined in the present study, and these geometries are illustrated in Figure 1: see Refs. 1, 2, or 3 for details of the experimental apparatus. The second and third sections below, respectively, describe the pressure asymmetries and their effect on $C_{w,min}$.

Pressure asymmetries

Generation of the asymmetries

A contraction with a 16:1 area ratio was fitted to the upstream end of the external flow annulus, as shown in Figure 2, and the inlet of the contraction was covered with wire mesh. By attaching sections of "honeycomb" to parts of the mesh, a number of different pressure distributions could be generated in the circumferential direction.

Figure 3 shows the circumferential variation of static pressure, measured at the 27 taps on the outside wall of the annulus, for six different patterns of pressure asymmetry. The measurements were obtained for seal 1 (the datum seal) with $G_c=0.01$, $Re_\theta=0$, and $Re_w=1.1\times10^6$. Only static pressures were measured, and no attempt was made to measure the variation of total pressure or secondary flow in the annulus. For further details of the flows in the annuli of turbomachinery, see Refs. 4 and 5.

The spectral distribution is different for each of the six pressure asymmetries, and one simple measure of the asymmetry is Δp_{max}, the maximum pressure difference between any two of the 27 taps. To give some idea of the asymmetry of the pressure distributions, it is convenient to define a pressure coefficient

$$C_{p,max}=\Delta p_{max}/\tfrac{1}{2}\rho\bar{W}^2 \quad (1)$$

The asymmetries created by the honeycomb sections are numbered 1 to 6 in order of increasing $C_{p,max}$, and Table 1 shows the values obtained for seal 1 with $G_c=0.01$, $Re_\theta=0$, and $Re_w=1.1\times10^6$. For the quasi-axisymmetric external flow discussed in II, the pressure asymmetries were caused mainly by small misalignments in the external flow passages and not by the deliberate introduction of disturbances into the flow. The quasi-axisymmetric case, referred to as asymmetry number 0, is also included in Table 1. It was found that $C_{p,max}$ was sensibly independent of Re_w and, for large values of Re_w, it was not significantly affected by the speed of the rotor.

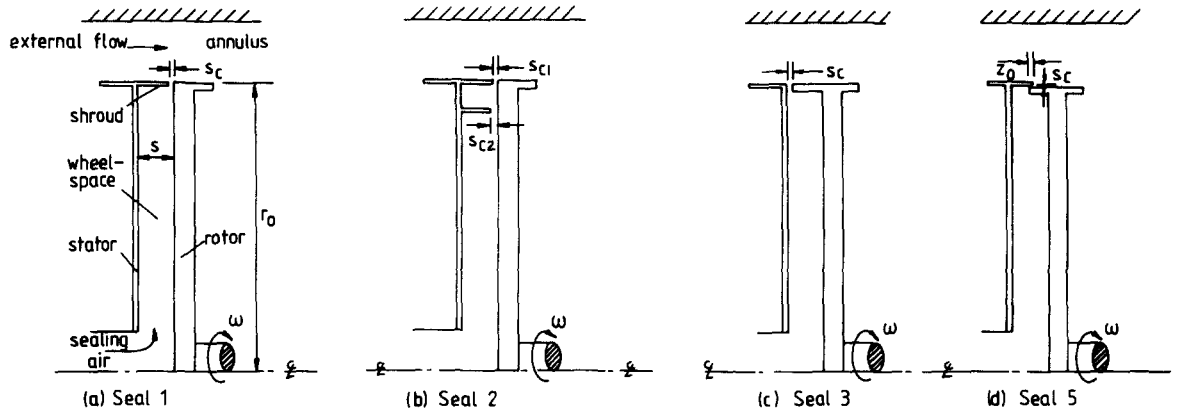

Figure 1 Simplified diagram of the four seals tested: (a) seal 1; (b) seal 2; (c) seal 3; (d) seal 5

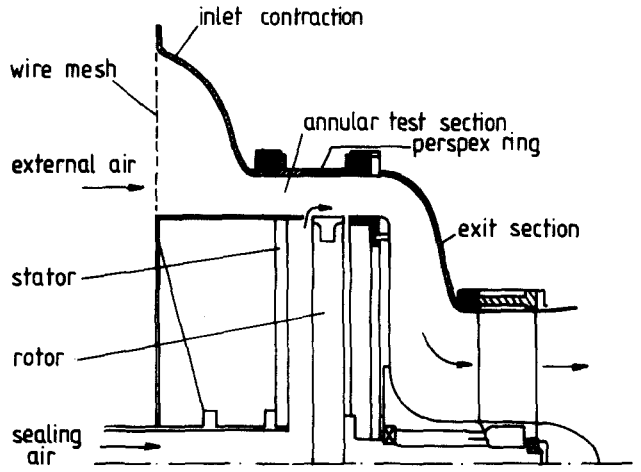

Figure 2 External-flow rig used for the asymmetry tests

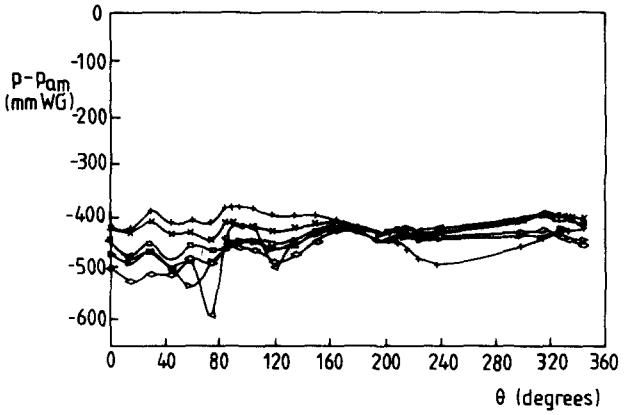

Figure 3 The circumferential variation of static pressure in the annulus for each of the six asymmetries: $C_w=0$, $Re_\theta=0$, $Re_w=1.1\times10^6$

Symbol	×	□	◇	▷	+	◁
Asymmetry number	1	2	3	4	5	6

The effect of the asymmetries on ingress

As reported in II, flow visualization revealed that, with an external flow, ingress could occur even when the rotor was stationary. Smoke introduced into the external flow showed that fluid moved transversely across the wheel space from regions of high to low pressure in the annulus. In the tests reported here, different asymmetries caused different effects with respect to the extent and direction of the ingested flow.

Figure 4 shows typical examples of the relationship between the observed flow patterns and the circumferential pressure distribution for seal 1 with $G_c=0.01$, $C_w=0$, $Re_\theta=0$, and $Re_w=1.1\times10^6$ for asymmetry numbers 3 and 5. It is apparent

Nomenclature

C_d	Discharge coefficient
$C_{p,max}$	$\Delta p_{max}/\frac{1}{2}\rho\bar{W}^2$
C_w	$\dot{m}/\mu r_o$, mass flow coefficient
G	s/r_o, gap ratio
G_c	s_c/r_o, seal clearance ratio
K	Empirical constant
$\dot{m}$	Mass flow rate of sealing air
p	Static pressure
P_{max}	$\frac{1}{2}C_{p,max}Re_w^2$
r	Radial distance from disk centerline
r_o	Outer radius of disk
Re_θ	$\rho\omega r_o^2/\mu$, rotational Reynolds number
Re_w	$\rho\bar{W}r_o/\mu$, axial flow Reynolds number
s	Axial gap between rotor and stator
s_c	Seal clearance
W	Axial component of velocity in the external-flow annulus
$\bar{W}$	Uniform value of W in inner part of annulus
Δp_{max}	Maximum circumferential pressure difference in annulus
Δp_s	Circumferentially averaged pressure drop across shroud
Δp_1	Local pressure drop across shroud
μ	Fluid viscosity
ρ	Fluid density
ω	Angular speed of rotor

Subscripts

min	Minimum value to prevent ingress
1, 2	Outer and inner shrouds (seal 2)
*	Values based on radius of inner shroud (seal 2)

Table 1 The value of $C_{p,max}$ for each of the asymmetries for seal 1 with $G_c=0.01$, $Re_\theta=0$, and $Re_w=1.1\times10^6$

Asymmetry number	0	1	2	3	4	5	6
$C_{p,max}$	0.067	0.10	0.18	0.20	0.22	0.22	0.48

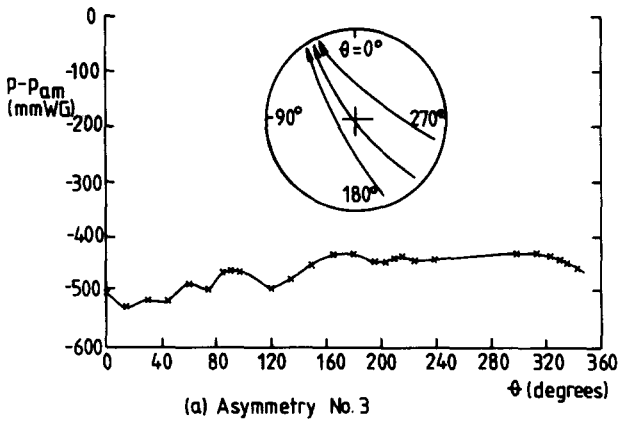

(a) Asymmetry No. 3

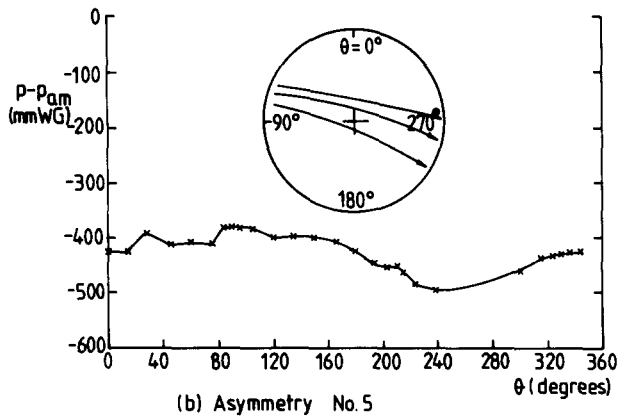

(b) Asymmetry No. 5

Figure 4 Observed flow patterns in the wheel space and circumferential variation of static pressure in the annulus for $C_w=0$, $Re_\theta=0$, $Re_w=1.1\times10^6$: (a) asymmetry no. 3; (b) asymmetry no. 5

that the flow direction in both cases is from the high- to the low-pressure region in the annulus: the wheel space acts as a short circuit to redress the balance of pressure in the annulus.

The above examples were for the case where $C_w=0$. If the cooling flow rate is increased, the amount of ingested fluid can be reduced and eventually ingress is prevented. Figure 5 shows sketches of the flow patterns deduced from flow visualization for seal 1 with $G_c=0.01$ and for seal 2, the double-shrouded seal, with $G_{c1}=G_{c2}=0.01$ for $Re_\theta=0$ and $Re_w=0.21\times10^6$. Referring to the diagrams for seal 1, note that at $C_w\simeq900$ the amount of ingestion is reduced and at $C_w\simeq1800$ it is virtually eliminated.

The patterns for seal 2 are different to those for seal 1: the outer wheel space provides a "ring road" that allows the transfer of most of the flow from the high- to the low-pressure regions in the external-flow annulus. In fact, at $C_w\simeq900$ no external flow enters the inner wheel space, and at $C_w\simeq1800$ all ingress has ceased. In the absence of external flow, it was shown in I that seal 2 had no particular merits compared with other seals. However, with external flow, seal 2 has the property of reducing ingress into the inner wheel space, and this could be used to obvious advantage in gas-turbine cooling systems.

From tests conducted for seal 2, it was found that pressure asymmetries measured on the stator between the two shrouds were much smaller than those measured on the outer wall of the annulus. As a consequence, the pressure asymmetry experienced by the fluid in the inner wheel space is significantly attenuated. As the magnitude of the pressure asymmetry affects the amount of ingestion that occurs, the inner wheel space is "buffered" by the second shroud.

Figure 6 shows the effect of C_w on the circumferential variation of Δp_1, where Δp_1 is the local pressure difference measured between a tap on the stator at $x=0.97$ and the corresponding tap on the outer wall of the annulus. The measurements were made for seal 1 with $G_c=0.01$, $Re_\theta=0$, and $Re_w=1.1\times10^6$, and the results for asymmetries 1, 3, and 5 are shown. It can be seen that, for all three cases, Δp_1 is negative at all circumferential locations for $C_w=0$. Increasing C_w causes an increase in the magnitude of Δp_1, but the circumferential distribution is virtually unaltered.

The distribution of Δp_1 is related to the ingestion observed by flow visualization, and the determination of $C_{w,min}$ is described below.

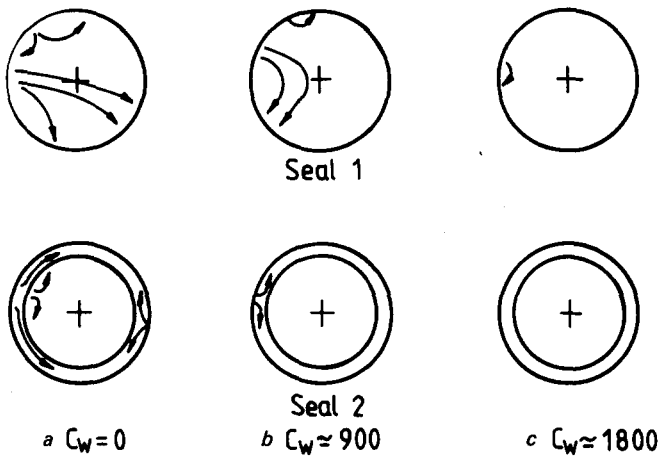

Figure 5 The effect of C_w on the observed flow patterns in the wheel space for $G_c=0.01$, $Re_\theta=0$, $Re_w=0.2\times10^6$: (a) $C_w=0$; (b) $C_w\simeq900$; (c) $C_w\simeq1800$

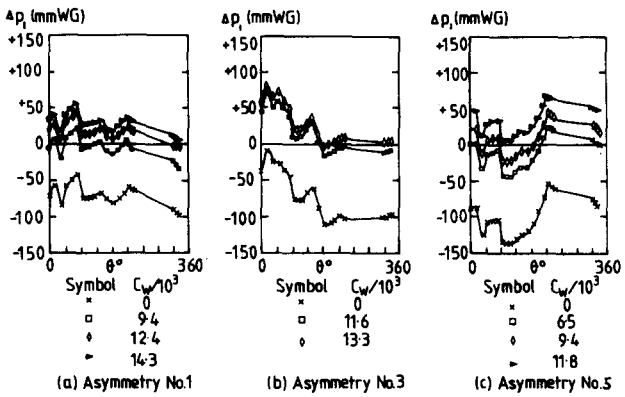

(a) Asymmetry No.1 (b) Asymmetry No.3 (c) Asymmetry No.5

Figure 6 The effect of C_w on the circumferential variation of pressure drop across seal 1 for $G_c=0.01$, $Re_\theta=0$, $Re_w=1.1\times10^6$: (a) asymmetry no. 1; (b) asymmetry no. 3; (c) asymmetry no. 5

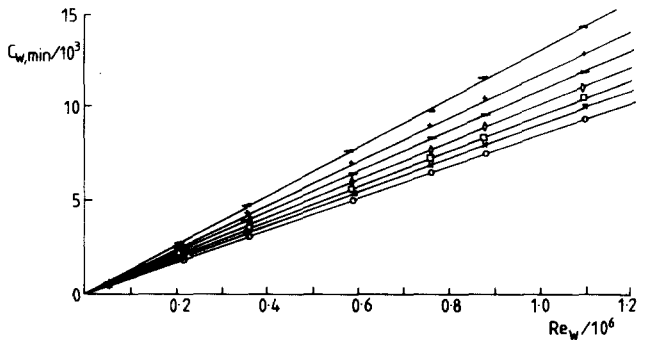

Figure 7 The variation of $C_{w,min}$ with Re_w for the different asymmetries: $G_c=0.01$, $Re_\theta=0$

Symbol	○	×	□	◇	▻	+	◅
Asymmetry number	0	1	2	3	4	5	6

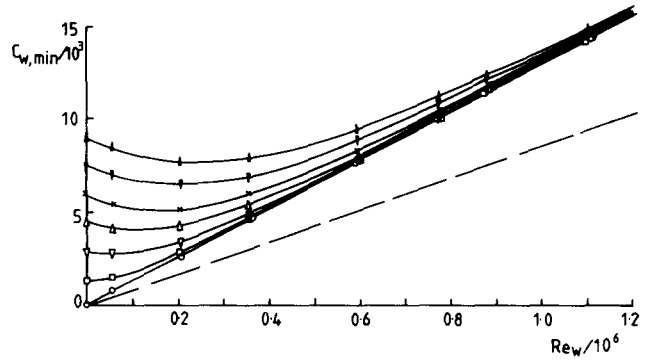

Figure 8 The effect of Re_θ on the variation of $C_{w,min}$ with Re_w for seal 1 with asymmetry number 6:

Symbol	○	□	▽	△	×	▼	▲
$Re_\theta/10^6$	0	0.2	0.4	0.6	0.8	1.0	1.2

Quasi-axisymmetric case ——————

The determination of $C_{w,min}$

Flow visualization

The flow visualization technique was the same as that described in I and II: smoke was injected into the external flow, and $C_{w,min}$ was taken to be the minimum value of C_w that prevented the appearance of smoke in the illuminated wheel space.

Figure 7 shows the variation of $C_{w,min}$ with Re_w for the quasi-axisymmetric case (number 0) and for each of the six asymmetries tested. The results, which were obtained for seal 1 with $G_c=0.01$ and $Re_\theta=0$, show that $C_{w,min}$ is proportional to Re_w and increases monotonically from asymmetry number 0 to number 6: that is, $C_{w,min}$ increases with increasing $C_{p,max}$ as well as with increasing Re_w.

Figure 8 shows the effect of Re_θ on the variation of $C_{w,min}$ with Re_w, for seal 1 with $G_c=0.01$, for asymmetry number 6. For comparison, a curve representing the average results for the quasi-axisymmetric case, with $Re_\theta=0$, is shown. For small values of Re_w/Re_θ the results show the sealing effect of the external flow: $C_{w,min}$ decreases with increasing Re_w. For large values of Re_w/Re_θ, in the external-flow-dominated regime, the effect of Re_θ is small and $C_{w,min}$ becomes proportional to Re_w. However, as discussed above, the value of $C_{w,min}$ required for asymmetry number 6 is significantly greater than that for the quasi-axisymmetric case.

The effect of Re_θ on the variation of $C_{w,min}$ with Re_w for the double-shrouded seal 2 with asymmetry number 4 is shown in Figure 9 for the case of $G_{c1}=G_{c2}=0.01$. In Figure 9(a), for the outer shroud, Re_θ and $C_{w,min}$ are based on the outer radius r_o; in Figure 9(b), for the inner shroud, Re_θ^* and $C_{w,min}^*$ are based on the radius r_o^* of the inner shroud ($r_o^*=0.9r_o$). For $Re_w=0$, there is little difference in performance between the two shrouds: $C_{w,min}$ and $C_{w,min}^*$ are proportional to Re_θ and Re_θ^*, respectively. For large values of Re_w, the value of $C_{w,min}$ for the outer shroud is much greater than that for the inner shroud. This is consistent with the results discussed in the previous section in which flow visualization revealed that the outer wheel space acted as a ring road that transported most of the ingested fluid.

Pressure measurements

Flow visualization showed that $C_{w,min}$ increased with increasing $C_{p,max}$, and a simple model for this behavior is presented below.

It is assumed that, in the external-flow-dominated regime, the circumferentially averaged pressure drop Δp_s across the shroud is related to the volumetric flow rate Q of the sealing air by

$$Q=C_d A(2\Delta p_s/\rho)^{1/2} \tag{2}$$

where $A=2\Pi r_o s_c$ is the area of the seal opening and C_d is a discharge coefficient. It follows from Equation 2 that

$$C_w=2\sqrt{2}\,\Pi C_d G_c(\rho\Delta p_s r_o^2/\mu^2)^{1/2} \tag{3}$$

and it is postulated that $C_w=C_{w,min}$ when $\Delta p_s=C\Delta p_{max}$, where C is an empirical constant. Hence

$$C_{w,min}=2\Pi K G_c P_{max}^{1/2} \tag{4}$$

where

$$K=\sqrt{2C}\,C_d \tag{5}$$

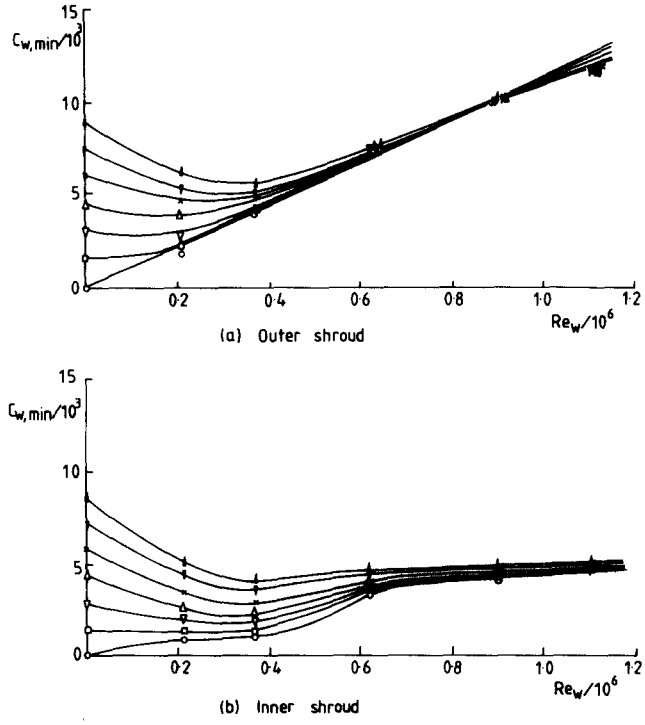

Figure 9 The effect of Re_θ on the variation of $C_{w,min}$ with Re_w for seal 2 with asymmetry number 0 for $G_c=0.01$; (a) outer shroud; (b) inner shroud

Symbol	○	□	▽	△	×	▼	▲
$Re_\theta/10^6$	0	0.2	0.4	0.6	0.8	1.0	1.2

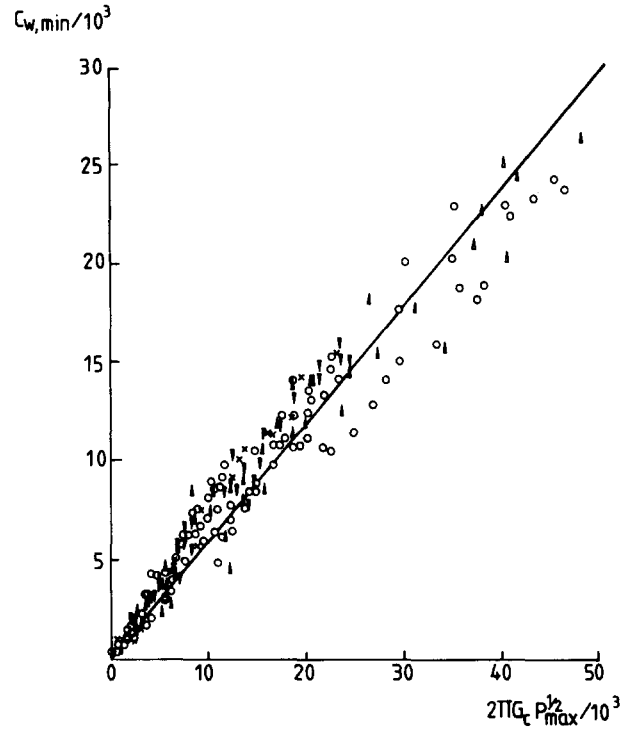

Figure 10 The variation of $C_{w,min}$ with $2\pi G_c P_{max}^{1/2}$
Symbol ○ × △ ▽
Seal 1 2 3 5
Equation 4 with $K=0.6$ ——————

and

$$P_{max} = \rho \Delta p_{max} r_o^2/\mu^2 = \tfrac{1}{2} C_{p,max} Re_w^2 \quad (6)$$

Figure 10 shows the variation of $C_{w,min}$ with the parameter $2\pi G_c P_{max}^{1/2}$. The measured values of $C_{w,min}$ were obtained by flow visualization for seals 1, 2, 3 and 5 (for seal 2, only the results for the outer wheel space are included) with $G_c = 0.005$, 0.01, and 0.02, $Re_\theta = 0$ and $Re_w \leqslant 1.1 \times 10^6$. Despite the scatter, the results are correlated reasonably well using a value of $K = 0.6$ in Equation 4. Since this equation takes no account of the seal geometry or of the spatial distribution of the pressure asymmetry, the results suggest that these effects may be of secondary importance and that P_{max} can be used to estimate $C_{w,min}$.

More tests need to be carried out with systematic variation of pressure and swirl in the external-flow annulus, but Equation 4 may prove to be helpful for design purposes in the external-flow-dominated regime. In the rotation-dominated regime, correlations of the form

$$C_{w,min} \propto G_c^m Re_\theta^n \quad (7)$$

were determined for the six different seal geometries in I. A conservative design would be one in which $C_{w,min}$ was assumed to be the greater of the values determined for the two regimes.

Conclusions

Six different circumferential distributions of static pressure have been used to separate the effects of flow rate and pressure asymmetry in the external-flow annulus of a shrouded rotating-disk system. Flow visualization revealed that, after ingress had occurred, ingested fluid moved transversely across the wheel space from regions of high to low pressure in the annulus. For seal 2, the double-shrouded seal, the outer wheel space between the two shrouds acted as a ring road allowing most of the ingested fluid to be transferred from regions of high to low pressure without crossing the inner wheel space.

In the external-flow-dominated regime, it was found that $C_{w,min}$ increased with increasing P_{max}, where P_{max} is the dimensionless maximum circumferential static pressure difference measured in the external-flow annulus. A simple correlation between $C_{w,min}$, G_c, and P_{max} was obtained for the four seal geometries tested with $G_c = 0.005$, 0.01, and 0.02 and $Re_w < 1.1 \times 10^6$. Using this correlation, together with correlations for the rotation-dominated regime studied in I, it should be possible to obtain a conservative estimate of $C_{w,min}$. From the results of the tests reported in this series of papers, it would appear that a double-shrouded radial clearance seal should have advantages over the other seal geometries in minimizing the amount of hot gas that is ingested into the wheel spaces of gas turbines.

It should be emphasized, however, that the above tests were conducted with spatially aperiodic pressure distributions. In a gas turbine, nozzles, and combustion chambers often create pressure disturbances that contain swirl and spatial periodicity. Attempts to model such disturbances, theoretically and experimentally, and to determine their effect on the "ingress problem" are continuing in the Thermo-Fluid Mechanics Research Centre at the University of Sussex.

Acknowledgments

The authors wish to thank Rolls Royce plc, Ruston Gas Turbines plc, and the Science and Engineering Research Council for sponsoring the work described in this series of papers. They are also indebted to Dr. J. R. Pincombe for his assistance with the flow visualization and to the technicians in the School of Engineering and Applied Sciences who manufactured the experimental apparatus.

References

1 Phadke, U. P. and Owen, J. M. Aerodynamic aspects of the sealing of gas-turbine rotor-stator systems, Part 1: The behaviour of simple seals in a quiescent environment. *Int. J. of Heat and Fluid Flow*, 1988, **9**(2), 98–105
2 Phadke, U. P. and Owens, J. M. Aerodynamic aspects of the sealing of gas-turbine rotor-stator systems, Part II: *Int. J. of Heat and Fluid Flow*, 1988, **9**(2), 106–112
3 Phadke, U. P. Aerodynamic aspects of the sealing of gas-turbine rotor-stator systems. D.Phil. thesis, University of Sussex, 1982
4 Greitzer, E. M. and Strand, T. Asymmetric swirling flows in turbomachinery annuli. *J. Eng. Power*, 1978, **100**, 618
5 Bry, P., Laval, P., and Billet, G. Distorted flow field in compressor inlet channels. *J. Eng. Gas Turbines Power*, 1985, **107**, 782